Magnetic breakdown in the semimetallic InAs/GaSb system

D. M. Symons
Grenoble High Magnetic Field Laboratory, MPI-FKF and CNRS, Boîte Postale 166, F-38042 Grenoble Cedex 9, France

M. Lakrimi and R. J. Nicholas
Clarendon Laboratory, Department of Physics, Oxford University, Parks Road, Oxford OX1 3PU, United Kingdom

D. K. Maude and J. C. Portal
Grenoble High Magnetic Field Laboratory, MPI-FKF and CNRS, Boîte Postale 166, F-38042 Grenoble Cedex 9, France

N. J. Mason and P. J. Walker
Clarendon Laboratory, Department of Physics, Oxford University, Parks Road, Oxford OX1 3PU, United Kingdom
(Received 9 February 1998)

In-plane magnetotransport measurements have been performed on semimetallic InAs/GaSb structures where the magnetic field is rotated with respect to the sample growth axis. It has been observed that superlattices behave in a distinctly different manner to structures with a single InAs layer. In particular, extra frequencies appear in the Shubnikov–de Haas oscillations beyond a critical angle of rotation. It is argued that this can be explained by considering the detailed band structure of the superlattice taking into account the miniband of the electrons, the anisotropy of the holes and the energy minigap produced at the anticrossing point between the electron and hole dispersion relations. Furthermore, it is found that the observation of any Shubnikov–de Haas oscillations requires magnetic breakdown because of the presence of the minigap which splits the Fermi surface into unconnected islands. [S0163-1829(98)09335-7]

I. INTRODUCTION

The broken gap InAs/GaSb system has received much attention recently concerning whether it truly shows semimetallic behavior. In long period superlattices the confinement energy of the electrons in the InAs lies below the confinement energy of the holes in the GaSb and charge will transfer between the layers. If we consider the in-plane carrier motion, the dispersion relations corresponding to the electrons and holes anticross and due to mixing of the bands a small minigap is formed. Altarelli pointed out that for a structure with equal electron and hole densities, the Fermi energy must lie in this minigap and semiconducting behavior will result.[1] It has almost always been possible however to interpret magnetotransport measurements within the semimetallic picture, ignoring the presence of the minigap.[2] Lakrimi *et al.* have shown that the in-plane dispersion of the holes is strongly anisotropic, leading to some indirect overlap of the bands despite the existence of local energy gaps.[3] Therefore, primarily metallic conduction is observed at low temperatures, which is the overriding reason why the first experimental evidence of this minigap has only recently been reported.[3,4]

When a structure containing a two-dimensional electron gas (2DEG) is placed in a tilted magnetic field, it is well known that the splitting of the Landau levels is determined only by the component of the field which is perpendicular to the plane of confinement, whereas the Zeeman splitting is dependent on the total magnetic field.[5] Tilted field magnetotransport measurements have proved to be a powerful and much used technique with which the relative magnitudes of the Zeeman and Landau splitting can be varied (see, for example, Ref. 6). By contrast, in a superlattice (SL) where the carriers are free to move in all three dimensions the splitting of the Landau levels is no longer independent of the in-plane magnetic field. In this paper, we present tilted field magnetotransport measurements of both two-dimensional (2D) single well and three-dimensional (3D) SL structures performed in a dilution fridge at 40 mK. The differences between the two cases are explained by considering the dispersion in the direction parallel to the SL axis.

II. EXPERIMENTAL DETAILS

A number of InAs/GaSb structures, both single wells of InAs surrounded by GaSb and superlattices, have been measured under rotation in a dilution fridge at 40 mK. The samples were grown using atmospheric pressure metal-organic vapor phase epitaxy (MOVPE).[7] The electron to hole density ratios for the samples are between 2 and 1.05, with electron and hole mobilities of order 5 and 0.5 m^2/Vs, respectively. A typical data set for a sample consists of the Hall and magnetoresistance traces measured at 40 mK for about 100 different angles. In this paper the angle of rotation is defined to be the angle between the field and the growth axis. It is possible to rotate the sample *in situ* through small angular increments without causing significant heating above base temperature. This paper will concentrate on the results obtained with a single quantum well of 300 Å of InAs surrounded by GaSb (OX963 but called QW in this paper) and also those from a 10 period superlattice with 190 Å of InAs and 210 Å of GaSb (OX2672 but called SL in this paper). The electron and hole densities and mobilities for the two samples, deduced from fitting the Hall resistivity curves to a

TABLE I. The layer thicknesses together with the fitted electron and hole densities and mobilities of the two samples are given. The values quoted for the SL sample are the densities per layer.

	Thickness (Å)		Density (10^{11} cm^{-2})		Mobility (m^2/Vs)	
Sample	GaSb	InAs	Electron	Hole	Electron	Hole
QW		300	7.5	4.4	4.9	0.50
SL	210	190	8.4	5.8	4.4	1.2

classical two carrier expression are shown in Table I. Both these samples have sufficiently thin InAs layers that only one electron subband is populated and have been chosen because they emphasize the observed differences between single layer structures and SLs. Other samples with larger layer thicknesses have been measured and these essentially mirror the same observations except for additional complications which can be attributed to the population of multiple electron subbands.

III. RESULTS

A. QW sample

Doubly differentiated magnetoresistance traces of the QW sample plotted against the perpendicular component of the magnetic field ($B_\perp$) are shown in Fig. 1. It is assumed that at low fields the oscillations in the resistance are solely due to magnetic quantization of the 2D electrons with little or no contribution from the holes in the structure. In addition, we assume that we are in the low field limit where neither the carrier densities nor the Fermi energy change appreciably with magnetic field. (For $B_\perp < 3$ T, the filling factor, $\nu > 10$.) Evidence for this is provided by Fourier transforms of the oscillations which show a single peak with a constant carrier density which agrees with the electron density given in Table I, which was deduced from fitting the measured Hall

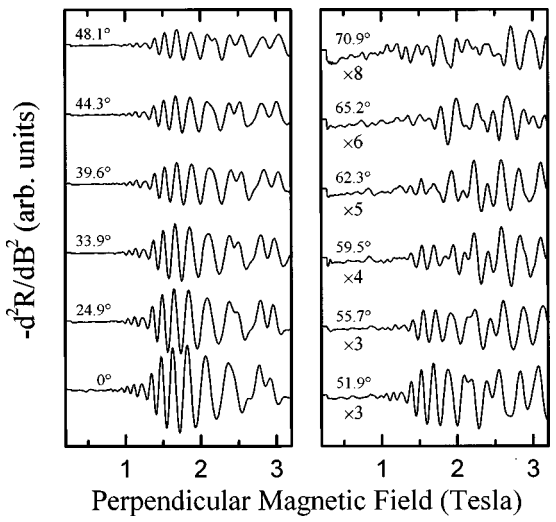

FIG. 1. The doubly differentiated longitudinal magnetoresistance traces of the QW sample measured at 40 mK are plotted against the perpendicular component of the applied magnetic field. The traces are labelled with the angle between the magnetic field and the growth axis and have been offset for clarity. The curves on the right have been expanded by the factors shown below the traces.

resistivity trace. The oscillations in the magnetoresistance remain at the same value of $B_\perp$ independent of the angle. The only change is that as the angle increases oscillations which appear at lower values of $B_\perp$ and hence correspond to larger filling factors become spin split. If θ is the angle between the applied magnetic field and the growth axis then the magnitude of the total magnetic field, B_T, for a given value of $B_\perp$ increases with $1/\cos\theta$. Since the Zeeman energy depends on B_T then as the angle increases the spin splitting should gradually become observable at lower values of perpendicular magnetic field.

As the angle of rotation increases the spin split minima gradually become deeper and for the trace measured at 62.3°, shown in Fig. 1, it is difficult to distinguish which minima are due to spin splitting and which to Landau splitting. At an angle of around 64° there is a phase change in the oscillations as the spin split minima become the deepest features. This phase change occurs at roughly the same angle of rotation for several different oscillations. It is difficult to give an accurate value for the angle at which this occurs because the oscillations are quite weak at these high angles of rotation. The angle for this phase change is defined by the Fang and Stiles criterion[5] as the angle at which the Zeeman splitting is half the size of the Landau splitting. This has often been used as a method to measure the effective g factor (see, for example, Ref. 8). Below this angle the higher energy spin state of the Nth Landau level is closest in energy to the opposite spin state of the same Landau level but beyond this angle it becomes closer to the lower energy spin state of the $(N+1)$th Landau level. This easily leads to the expression below for the effective g factor

$$g^* = \frac{m_0 \cos\theta}{m_e^*}, \tag{1}$$

where θ is the critical angle, m_e^* is the electron effective mass at the Fermi energy, and m_0 is the free electron mass. For this structure $m_e^* = 0.031 m_0$ giving a g^* of approximately 14. This is slightly less than the bulk value of 15,[9] because of nonparabolicity of the electron dispersion. Chang *et al.* have measured values between 17 and 23 for similar structures with much wider InAs layers[10] where nonparabolicity is much less important and the measured g^* could be enhanced by many-body effects. Smith and co-workers measured values between 7.8 and 8.7 in a much thinner InAs well,[11] where the confinement energy is a long way above the band edge and nonparabolicity greatly reduces the g factor. It is not our intention in this paper to measure an accurate value for the electron g factor. The purpose of the approximate value deduced here is to rule out any effects of spin splitting in the discussion of the experimental data obtained from the SL sample which follows.

Fourier transforms (FTs) of the QW data have been performed for all the measured angles of rotation. All of these show a single peak indicating that only one electron subband is occupied. This peak remains at almost the same position when expressed in terms of the perpendicular component of the magnetic field, as shown in Fig. 2, indicating that the electron gas is truly two dimensional. It is important to note here that even at large angles when spin splitting of the fea-

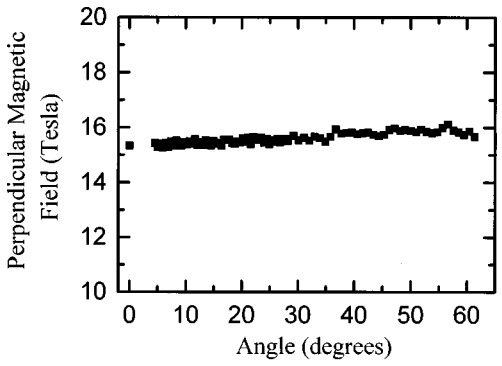

FIG. 2. FTs of the magnetoresistance oscillations of the QW sample have been performed and the positions of the peaks are plotted as a function of angle. The peak positions are given in terms of the perpendicular component of the magnetic field. For each angle the FT has been performed over the same range of values of the perpendicular component of the magnetic field, namely 0.5 to 5.0 T.

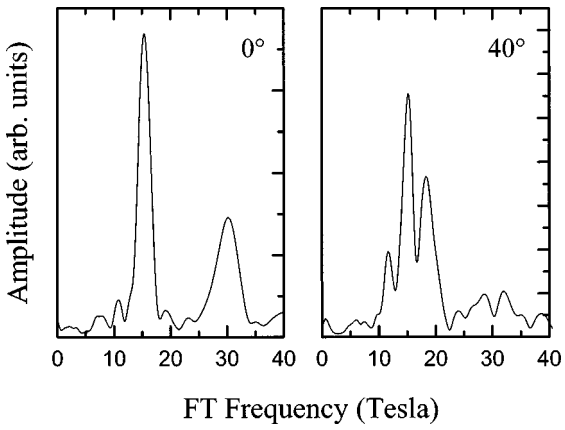

FIG. 4. FTs of the magnetoresistance oscillations of the SL sample are shown for two angles. At 0° there is a single peak at about 15 T, plus its harmonic at ~30 T, but at 40° an additional peak appears at a slightly higher frequency than the first peak as well as a third weaker peak.

tures is very pronounced, there is still only one fundamental frequency of oscillations in the FT. The appearance of spin splitting only changes the shape of the oscillations leading to sharpening and splitting of the peaks. The periodicity of the oscillations is not changed and therefore the spin splitting cannot introduce extra frequencies into the oscillations. The only effect it can have on the FTs of the data is that the relative amplitudes of the harmonics are changed.

B. SL sample

It is clear from even a quick glance at the raw data of the SL sample shown in Fig. 3 that this sample behaves in quite a different manner to the QW sample described in the previous section. As for the QW sample, it is assumed initially

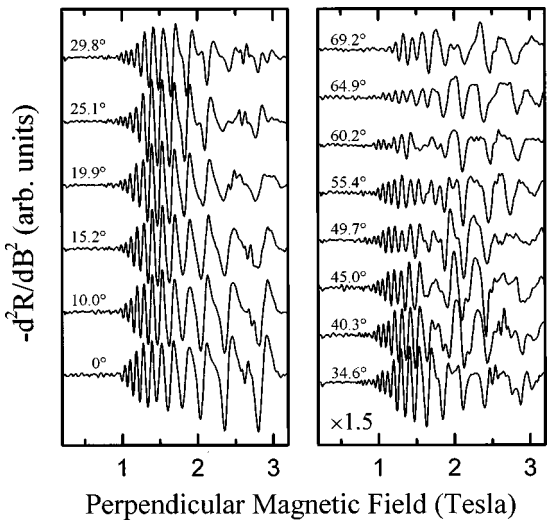

FIG. 3. The doubly differentiated longitudinal magnetoresistance traces of the SL sample measured at 40 mK are plotted against the perpendicular component of the applied magnetic field. The traces are labelled with the angle between the magnetic field and the growth axis and have been offset for clarity. The curves on the right have been expanded by a factor of 1.5.

that the oscillations at low field are solely due to the magnetic quantization of the electrons, with little effect from the holes in the structure. The role that the holes play in the observed behavior will become clear later in the paper. It can be seen from Fig. 3 that at angles up to about 33°, the low field oscillations remain quite constant when plotted as a function of the perpendicular component of the magnetic field. The only significant change is that the spin splitting becomes resolved at lower fields as the angle increases. At angles greater than 33° however, there is a significant change in the character of the oscillations. Many new features appear, especially in the region of field above 1.5 T, and these evolve rapidly as the sample is rotated further away from 0°. This is in marked contrast to the behavior observed for the QW sample which is shown in Fig. 1. The g factor of the electrons in this structure must have a similar value to that deduced for the QW sample, since the widths of the InAs layers in the two samples and their electron densities are very similar. As explained in the previous section, the Fang and Stiles criterion will not be fulfilled until the angle reaches approximately 64° so the observed change in the oscillations at 33° cannot be due to spin splitting. In any case, the change in character of the oscillations looks very different from the phase change observed for the QW sample at 64° in Fig. 1.

The change in character of the low field oscillations at an angle of about 33° is clearly demonstrated by the FTs of the oscillations which are shown in Figs. 4 and 5. At small angles there is only one peak in the FTs, plus a harmonic at twice the frequency which is also plotted in Fig. 5. The fundamental peak remains at a constant value of the perpendicular component of the magnetic field as the sample is rotated, suggesting that the Fermi surface is cylindrical. At an angle of about 33° there is a dramatic change and extra frequencies appear in the FT, which persist until the largest angles shown. The peak at about 18.5 T, a slightly larger frequency than that of the peak observed at small angles of rotation is the strongest of the extra peaks but additional weaker peaks are also included in the figure. At about 70° the amplitude of the oscillations in the raw traces becomes too small and the FTs are no longer very clear. These extra frequencies cannot

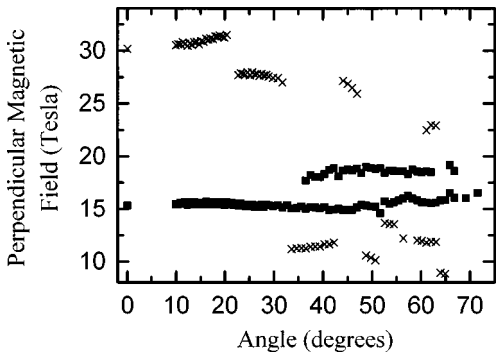

FIG. 5. FTs of the magnetoresistance oscillations of the SL sample have been performed and the positions of the peaks are plotted as a function of angle. The peak positions are given in terms of the perpendicular component of the magnetic field. The stronger peaks are plotted as squares and the weaker peaks as crosses. For each angle the FT has been performed over the same range of values of the perpendicular component of the magnetic field, namely 0.5 to 5.0 T.

be produced by spin splitting, since they are not harmonics of the fundamental frequency. Both this SL sample and the QW sample described previously have only one electron subband occupied. The only major difference between these samples is that the SL sample has ten active layers whereas the QW sample has only one. The unusual behavior of the SL sample is therefore most likely to be due to wavefunction overlap between the layers which will lead to an electron miniband and nonzero dispersion along the SL axis. We will therefore consider this in the next section.

IV. DISCUSSION

A. Corrugation of the electron Fermi surface

Eight-band $k\cdot p$ calculations of the SL sample suggest that the electron miniband width, Δ, should be of order 15 meV.[12] This means that at the edge of the Brillouin zone, where $k_z=\pm\pi/d$, the confinement energy is closer to the Fermi energy than at the center of the Brillouin zone where $k_z=0$. The growth axis is aligned along the z direction and d is the period of the SL. The Fermi wave vector measured perpendicular to the k_z axis is therefore smaller at $k_z=\pm\pi/d$ than at $k_z=0$ and the Fermi surface is a corrugated cylinder as shown in Fig. 6. Yamaji has explained the angular dependent magnetoresistance oscillations observed in organic superconductors by considering a similar corrugated cylindrical Fermi surface.[13]

In the structures studied here the electron and hole densities are almost equal, but the dominant contribution to the conduction is provided by the electrons because they have a larger mobility. For the moment, therefore, we will ignore any effects from the holes and just consider the motion of electrons on this corrugated Fermi surface when a small magnetic field is applied in an arbitrary direction. The electrons will perform orbits of constant energy which are constrained to planes perpendicular to the magnetic field. It is well known that the only orbits which will give rise to oscillations in the magnetoresistance are the extremal orbits around the Fermi surface. The frequency of the oscillations, which are periodic in $1/B$, is proportional to the k space area

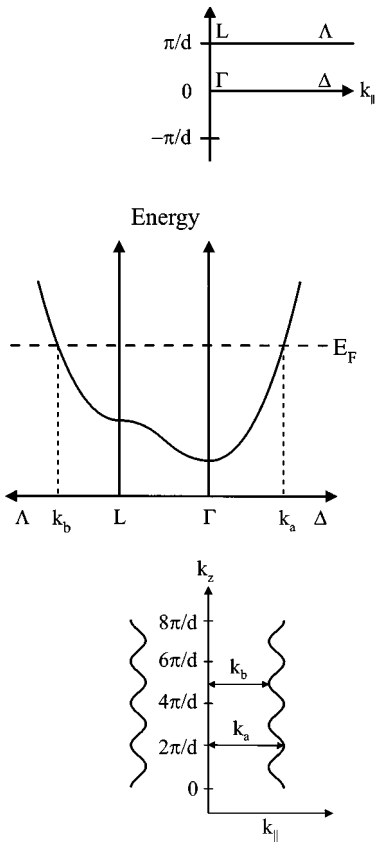

FIG. 6. The dispersion relations of the electrons are shown for both the in-plane and out-of-plane directions. The Brillouin zone nomenclature is shown at the top of the figure. The Fermi wave vector measured perpendicular to the SL axis is larger at $k_z=0$ (k_a) than at $k_z=\pm\pi/d$ (k_b), which leads to a corrugated cylindrical Fermi surface as depicted in the lower part of the figure.

of the orbit. When the magnetic field is applied parallel to the SL axis it is clear that there are two extremal area orbits. The orbit with maximum area lies in the plane $k_z=0$ and the orbit with minimum area lies in the plane $k_z=\pm\pi/d$. Figure 7 shows how the calculated oscillation frequencies corresponding to these extremal Fermi surface orbits vary as the angle between the magnetic field and the SL axis is varied. At particular angles, ϕ, all the orbits have the same area. These angles are described by the expression

$$\tan\phi=\frac{\left(n-\frac{1}{4}\right)\pi}{dk_F}, \tag{2}$$

where n is a positive nonzero integer and k_F is the Fermi wave vector.[13]

We might therefore expect to see two peaks in the FTs of the SL sample when the magnetic field is applied perpendicular to the layers and furthermore the positions of these peaks would oscillate and cross each other as the sample is rotated. This is indeed very much like the behavior reported previously by Chang *et al.* in a 1000-Å period SL.[10] These early InAs/GaSb samples tended to have a large excess of electrons over holes and therefore we would expect significantly different behavior to the structures studied in this paper which are close to the ''intrinsic'' limit. For the SL

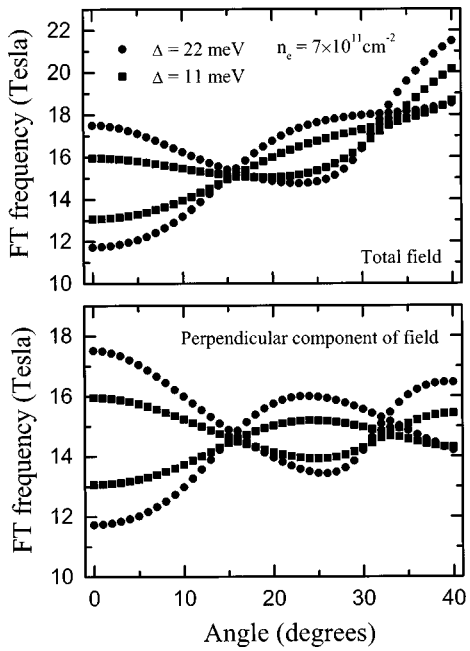

FIG. 7. The calculated frequency of the Shubnikov–de Haas oscillations, corresponding to the extremal areas of the Fermi surface are plotted as a function of the angle of the applied magnetic field. In the upper plot the frequencies are given in terms of the total applied field whereas in the lower plot they are given in terms of the perpendicular component of the field. The calculation is for a 400 Å period SL with an electron density of 7×10^{11} cm^{-2} and two values of the miniband width, Δ.

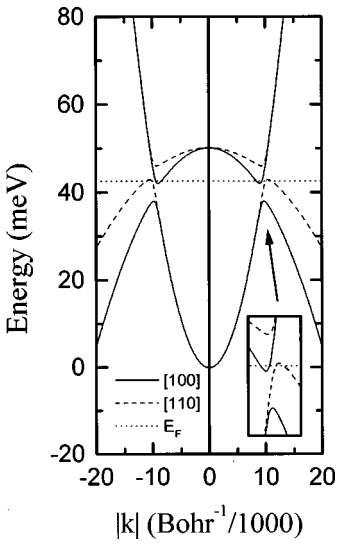

FIG. 8. The dispersion relations are shown for two different directions of the in-plane wavevector, [100] and [110]. Away from $k=0$, the dispersion relations of the electrons and holes mix and a minigap opens up close to the anticrossing point. Since the hole mass is anisotropic the minigap lies at a different energy for different directions of the in-plane k vector. The highest energy points of the lower M-shaped band lie above the lowest energy points of the upper W-shaped band. The inset shows that both bands cross the Fermi energy and therefore there is a Fermi surface.

sample we do see more than one frequency in the oscillations but only for angles beyond the critical angle of 33°. This suggests that we need to look beyond this ''Yamaji'' picture of the corrugated Fermi surface to fully explain the data presented here. The SL sample we have used in this work has comparable electron and hole densities and therefore the Fermi surface is close to the point where the electron and hole in-plane dispersions anticross. Recently, it has been found that the mixing between the electrons and holes can be very important and sometimes it is imperative to take this into account in order to understand the observed behavior.[3] Hence, in the next section we will consider what role the holes play in the band structure of the SL.

B. Mixing between the electrons and holes

In semimetallic InAs/GaSb structures the in-plane electron and heavy hole dispersion relations anticross and a minigap of order 7 meV opens up between the lower M-shaped band and the upper W-shaped band which are shown in Fig. 8. The dispersion relations shown in this figure were calculated using the two-band model which is introduced later in this section. The presence of this minigap was predicted theoretically[1] a long time ago but has only recently been observed experimentally.[3,4] If the electron and hole densities are equal then the Fermi energy must lie in the minigap and we would expect the sample to show semiconducting behavior. In practice any structure exhibits primarily metallic conduction if the electron and hole confined levels overlap at $k=0$, showing that there is still an overlap between the M- and W-shaped bands. The in-plane hole mass is larger in the [110] direction than in the [100] direction and therefore the minigap lies at a different energy for different directions of the in-plane k vector. This is sufficient to produce a band overlap, shown in the inset to Fig. 8, which leads to semimetallic behavior in all but the very thinnest structures.[3] Furthermore, the large negative magnetoresistance observed in these structures when the magnetic field is applied parallel to the layers is described well by a model incorporating the presence of the minigap and the hole anisotropy.[14]

Eight-band $k\cdot p$ calculations show that for the SL sample the width of the electron miniband should be of order 15 meV.[12] There is strong mixing between the electrons confined in the InAs layers and the light holes confined in the GaSb layers and this acts to enhance the overlap of the electron wave functions between neighboring wells. The wave function of the heavy holes does not penetrate very far into the InAs layers and hence there is almost no dispersion of the holes in the direction perpendicular to the layers. Consequently, the hole miniband width is very close to zero. In addition, the calculations show that the minigap produced by the mixing of the electrons and holes is very dependent on the superlattice wave vector, k_z. In particular, it is much larger at $k_z=0$ than at $k_z=\pm\pi/d$.

The approximate shape of the SL Fermi surface has been calculated and various cross sections are shown in Fig. 9. In addition the Fermi surface is shown as a three-dimensional solid object in Fig. 10. A two-band model is used which consists of an electron band with parabolic in-plane dispersion and a heavy hole band with anisotropic in-plane dispersion. This is the same as the model used previously[3,14] but extended to include the dispersion along the SL axis. The energies of the carriers are given by

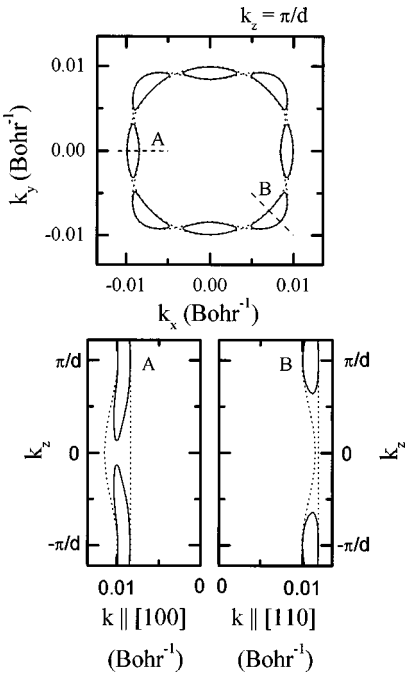

FIG. 9. The Fermi surface of the SL sample is calculated using an electron miniband width of 15 meV and a minigap which varies with the SL wave vector. The top plot shows a cross section in the (k_x,k_y) plane. The bottom plots show the cross sections of the Fermi surface islands labeled A and B in the $(k_\parallel,k_z)$ plane with $k_\parallel$ along [100] for island A and [110] for island B. The vertical axes of the bottom plots have been expanded, $\pi/d=0.0042$ Bohr^{-1}. The Fermi surface is split up into unconnected islands with gaps between these islands both perpendicular and parallel to the SL axis. To demonstrate the effect of the mixing, dotted lines show the Fermi surface in the absence of any electron-hole mixing.

$$E_{\pm}(k_x,k_y,k_z) = \tfrac{1}{2}\{E_e^0(k_x,k_y,k_z)+E_h^0(k_x,k_y) \pm \sqrt{[E_e^0(k_x,k_y,k_z)-E_h^0(k_x,k_y)]^2+[\delta(k_z)]^2}\}, \tag{3}$$

where $E_e^0(k_x,k_y,k_z)$ and $E_h^0(k_x,k_y)$ are the electron and hole energies of the uncoupled system and $\delta(k_z)$ is the minigap or coupling energy which is varied sinusoidally from a maximum value at $k_z=0$ to a minimum at $k_z=\pm\pi/d$. The isotropic electron band is given by

$$E_e^0(k_x,k_y,k_z)=E_e^z(k_z)+\frac{\hbar^2(k_x^2+k_y^2)}{2m_e^*}, \tag{4}$$

where the electron effective mass, m_e^*, is taken as $0.030\,m_0$ to account for nonparabolicity and $E_e^z(k_z)$ is the dispersion of the electrons along the SL axis which is chosen to be sinusoidal. The warped hole band, which is independent of k_z, is given by

$$E_0^h(k_x,k_y)=E_g-\frac{\hbar^2}{m_0}\{A(k_x^2+k_y^2)-[B^2(k_x^2+k_y^2)^2 + C^2k_x^2k_y^2]^{1/2}\}, \tag{5}$$

where E_g is the energy difference between the electron and hole confinement energies at zero wave vector and the constants A, B, and C are taken to be 14.3, 10.4, and 13.5, respectively, and control the mass and anisotropy of the hole dispersion. The position of the Fermi energy, E_F, is chosen to give the correct values for the electron and hole densities, n_e and n_h, in the absence of electron-hole mixing and with zero dispersion of the electrons along the SL axis. This leads to the expression

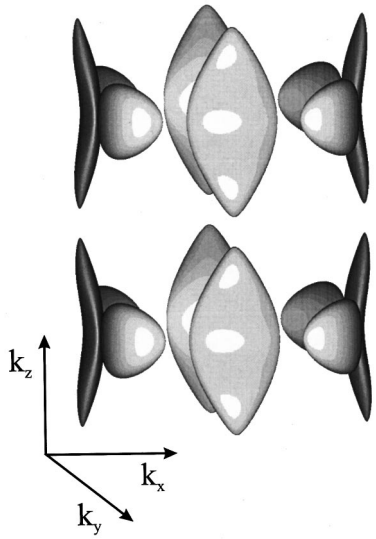

FIG. 10. Two Brillouin zones of the Fermi surface of the SL sample are shown drawn as a three dimensional solid object. As for Fig. 9 the k_z axis has been expanded. The light is shining from in front of the object so that surfaces parallel to the plane of the paper are white and surfaces perpendicular to the page are dark.

$$E_F=\frac{\hbar^2\pi n_e}{m_e^*}=E_g-\frac{\hbar^2\pi n_h}{m_h^*}, \tag{6}$$

where m_h^* is an average in-plane mass for the holes. The shape of the Fermi surface can then be calculated by finding the points in k space for which $E_{\pm}(k_x,k_y,k_z)=E_F$.

It is perhaps wise at this point to consider which orbits on the Fermi surface give rise to the Shubnikov–de Haas oscillations which we observe. Figure 9 shows the cross-section of the Fermi surface of the SL in a (k_x,k_y) plane. The Fermi surface of the QW sample will be very similar. The Fermi surface consists of several unconnected islands. When a magnetic field is applied, carriers will perform orbits of the closed areas of the Fermi surface. As the strength of the magnetic field is increased the rate at which the carriers perform these orbits increases, simply because the cyclotron frequency is proportional to the magnetic field. As a rough guide, Shubnikov–de Haas oscillations should begin to be observed when a carrier is able to perform a complete orbit without scattering. For each of the closed orbits in the Fermi surface of Fig. 9, half of the states are very holelike and hence are associated with a larger mass. The cyclotron frequency is inversely proportional to the effective mass and therefore the carrier will take a relatively long time to complete the holelike part of the orbit. It is very likely that the carrier will scatter and hence no oscillations are observed with a frequency which corresponds to the area of these closed orbits. If the magnetic field is large enough then there

will be a significant probability that a carrier is able to tunnel across the gaps in k space between the unconnected islands of the Fermi surface. This is termed magnetic breakdown.[15] A carrier is then able to perform a complete orbit, while remaining in electronlike states. The k-space area of this orbit is very close to that of the electron Fermi surface in the absence of any mixing between the electrons and holes. It is this area which corresponds to the frequency of the oscillations that we observe in the resistance.

It is interesting to note that for many intrinsic InAs/GaSb structures which typically have mobilities, μ, as high as 10 m^2/Vs, the oscillations are very rarely observable below 1 T. For the SL sample studied here the electron mobility of 4.4 m^2/Vs quoted in Table I has been determined from the resistance at zero magnetic field. However, it has been suggested that the ''true'' electron mobility should be determined from the resistance in the presence of a large parallel magnetic field.[14] At zero field the group velocities of the carriers at the Fermi energy are reduced by the presence of the minigap, but the application of a parallel magnetic field shifts the electron and hole dispersion relations apart in k space and removes the effects of the minigap. For the SL sample described in this paper the mobility determined from the resistance in a large parallel magnetic field is 12.7 m^2/Vs, which leads to a transport lifetime, τ_c, of 2.2 ps. A simple estimate of the quantum lifetime, τ_q, provided by looking at the field at which the oscillations start gives a value of 0.18 ps. It is well known that these two lifetimes are not, in general, equal, since small angle scattering events will effect the observation of Shubnikov–de Haas oscillations, but will have little effect on the measured resistance. The ratio τ_c/τ_q depends on the dominant scattering mechanism, however, in these samples we would expect this ratio to be close to unity since it is thought that interface roughness scattering is the dominant mechanism.[16] This contradiction can be resolved by assuming that magnetic breakdown only occurs above a perpendicular field of 1 T and this always prevents any oscillations being observed at lower fields.

A naive estimate of the field at which magnetic breakdown occurs is provided by comparing the sizes of the cyclotron energy ($\hbar\omega_c$) and the minigap (~ 7 meV[3]). At a field of 1 T the magnetic energy is 4 meV, which is the same order of magnitude as the minigap. Hu and MacDonald have calculated the breakdown fields for two parallel 2DEGs placed in a tilted magnetic field[17] which is quite similar to the situation presented in this paper. They find that the perpendicular component of the magnetic field at which breakdown occurs is such that the magnetic energy is comparable with the size of the minigap and also that it depends on the magnitude of the parallel component of the field. Therefore the breakdown field varies with the angle between the sample axis and the applied field. Harff *et al.* present experimental results of $GaAs/Al_xGa_{1-x}As$ double quantum well samples in tilted fields where they find that the perpendicular component of the magnetic field required for breakdown is between 0.3 and 1.2 T.[18] The energy gap in their study is smaller (2 meV) but their electron mass is larger so we would expect the breakdown field in their structures to be of the same order of magnitude as the samples studied in this paper.

In the previous section when we considered the corrugated electron Fermi surface without any effects from the holes, it was the orbit centered around the $k_z=0$ plane which gave rise to the oscillations with the larger frequency. Figure 9 shows that there is no Fermi surface in the $k_z=0$ plane for the SL. The Fermi energy lies in the gap between the W- and M-shaped bands for all directions of the in-plane k vector. When a magnetic field is applied along the SL axis there is no longer an allowed orbit whose area in k space is close to the previous maximum. Of course, there is still an orbit which has a maximum area. This will not give rise to Shubnikov–de Haas oscillations though, since there will not be a large peak in the number of orbits which have this particular area. Therefore we would expect to see only one frequency in the FTs of the oscillations for small angles of rotation corresponding to the extremal orbits close to the $k_z=\pm\pi/d$ plane, where magnetic breakdown occurs at low field values. For a constant value of $B_\perp$ the total magnetic field increases as the angle increases. At a particular angle the total field will be large enough that magnetic breakdown will occur in the $k_z=0$ plane of the Fermi surface and orbits with a larger area giving rise to oscillations with a higher frequency will become possible. The field required for magnetic breakdown in the $k_z=0$ plane will be larger than that for the $k_z=\pm\pi/d$ plane because the minigap is larger. Hence, the form of the calculated Fermi surface of the SL suggests that for small angles there should be only one frequency in the oscillations, but a second higher frequency should appear when the sample is rotated beyond a particular angle. This is in good qualitative agreement with the observed behavior of the SL sample.

The two strong peaks in the FTs of the SL are due to the maximum and minimum area orbits. The frequencies of these orbits are proportional to their areas in k space. We can use the difference in these areas to deduce an approximate value of 11 meV for the miniband width of the electrons. This is in good agreement with the value of ~ 15 meV calculated using an eight-band $k\cdot p$ model.[12] One possible objection to the explanation given above is that in the previous section it was shown that for a corrugated electron Fermi surface the frequency of the oscillations expressed in terms of the perpendicular component of the magnetic field should vary as the sample is rotated, but in Fig. 5 the peak remains at almost a constant value. It should be noticed from Fig. 9 that the presence of the minigap acts to make the Fermi surface more cylindrical, reducing the corrugation produced by the dispersion of the electrons along the SL axis. This is a possible explanation why the peaks in the FTs of the SL remain at almost a constant value when the sample is rotated.

When the angle of the magnetic field is greater than $\tan^{-1}(\pi/dk_F)$ then every possible Fermi surface orbit will extend over more than one Brillouin zone along the k_z direction. This means that all orbits must include some states in the region close to the $k_z=0$ plane where there is no Fermi surface. This happens at $\sim 22°$ for the SL sample studied here. The lower frequency oscillations do not disappear beyond this angle so the carriers must be able to tunnel through the gaps in the Fermi surface close to the $k_z=0$ plane. Since magnetic breakdown is occurring in this plane, we must consider the question of why the second frequency only appears in the oscillations when the angle exceeds 33°. In fact, there

are two reasons why no carriers perform orbits in this plane when the magnetic field is applied parallel to the SL axis. There are no allowed orbits and in addition the density of states at the Fermi surface is zero. Carriers perform orbits of the Fermi surface until they are scattered to another point on the Fermi surface, but they are never scattered to any points close to the $k_z=0$ plane because the density of states is zero. Hence even when there is significant magnetic breakdown and a carrier is able to perform an orbit with the maximal k-space area, it is unlikely that it will be scattered into a state in order to begin this orbit because the density of states is small.

V. CONCLUSIONS

We have presented tilted magnetotransport measurements of both a QW sample and a SL sample which show distinctly different behavior. The QW sample shows classic 2D electron gas behavior, whereas the SL sample shows a complex series of oscillating features with two strong periodicities once the sample is rotated beyond 33°. It is seen that magnetic breakdown is required in order to observe any oscillations in the resistance, which explains why oscillations do not start before ~ 1 T even for the highest mobility samples. The shape of the SL Fermi surface has been calculated and it is seen that there is no Fermi surface in the $k_z=0$ plane. There is no allowed orbit with maximal area and therefore only one frequency in the oscillations for small angles. For larger angles, the total magnetic field is larger and because of magnetic breakdown the frequency corresponding to the maximum area orbit appears in the oscillations.

ACKNOWLEDGMENT

D.M.S. acknowledges the support of the TMR program of the European Union.

[1] M. Altarelli, Phys. Rev. B **28**, 842 (1983).
[2] E. E. Mendez, L. Esaki and L. L. Chang, Phys. Rev. Lett. **55**, 2216 (1985); M. S. Daly, K. S. H. Dalton, M. Lakrimi, N. J. Mason, R. J. Nicholas, M. van der Burgt, P. J. Walker, D. K. Maude and J. C. Portal, Phys. Rev. B **53**, R10 524 (1996).
[3] M. Lakrimi, S. Khym, R. J. Nicholas, D. M. Symons, F. M. Peeters, N. J. Mason and P. J. Walker, Phys. Rev. Lett. **79**, 3034 (1997).
[4] M. J. Yang, C. H. Yang, B. R. Bennett and B. V. Shanabrook, Phys. Rev. Lett. **78**, 4613 (1997).
[5] F. F. Fang and P. J. Stiles, Phys. Rev. **174**, 823 (1968).
[6] A. Schmeller, J. P. Eisenstein, L. N. Pfeiffer and K. W. West, Phys. Rev. Lett. **75**, 4290 (1995); P. J. Gee, F. M. Peeters, J. Singleton, S. Uji, H. Aoki, C. T. B. Foxon and J. J. Harris, Phys. Rev. B **54**, R14 313 (1996).
[7] G. R. Booker *et al.*, J. Cryst. Growth **145**, 778 (1994); **146**, 495 (1995).
[8] J. C. Portal, R. J. Nicholas, M. A. Brummell, M. Razeghi and M. A. Poisson, Appl. Phys. Lett. **43**, 293 (1983); R. J. Nicholas, M. A. Brummell, J. C. Portal, K. Y. Cheng, A. Y. Cho and T. P. Pearsall, Solid State Commun. **45**, 911 (1983).
[9] C. R. Pidgeon, D. L. Mitchell and R. N. Brown, Phys. Rev. **154**, 737 (1967).
[10] L. L. Chang, E. E. Mendez, N. J. Kawai and L. Esaki, Surf. Sci. **113**, 306 (1982).
[11] T. P. Smith III and F. F. Fang, Phys. Rev. B **35**, 7729 (1987).
[12] T. A. Vaughan, Doctorate of Philosophy thesis, University of Oxford, 1996, Chap. 7 (unpublished).
[13] K. Yamaji, J. Phys. Soc. Jpn. **58**, 1520 (1989).
[14] D. M. Symons, F. M. Peeters, M. Lakrimi, S. Khym, J. C. Portal, N. J. Mason, R. J. Nicholas, and P. J. Walker, Physica E **2**, 353 (1998).
[15] D. Shoenberg, *Magnetic Oscillations in Metals* (Cambridge University Press, 1984).
[16] K. P. Martin, R. J. Higgins, J. J. L. Rascol, H. Yoo and J. R. Arthur, Surf. Sci. **196**, 323 (1988).
[17] J. Hu and A. H. MacDonald, Phys. Rev. B **46**, 12 554 (1992).
[18] N. E. Harff, J. A. Simmons, G. S. Boebinger, J. F. Klem, L. N. Pfeiffer and K. W. West, in *Proceedings of the 23rd International Conference on the Physics of Semiconductors*, edited by M. Scheffler and R. Zimmermann (World Scientific, Singapore, 1996), Vol. 3, p. 2199.